Families of cut-graphs for bordered meshes with arbitrary genus

G. Patanè M. Spagnuolo B. Falcidieno [1]

Abstract

Given a triangulated surface $\mathcal{M}$ with arbitrary genus, the set of its cut-graphs depends on the underlying topology and the selection of a specific one should be guided by the surface geometry and targeted applications. Most of the previous work on this topic uses mesh traversal techniques for the evaluation of the geodesic metric, and therefore the cut-graphs are influenced by the mesh connectivity. Our solution is to build up the cut-graph on the iso-contours of a function $f : \mathcal{M} \to \mathbb{R}$, that cut the topological handles of $\mathcal{M}$, and on the completion of the cut-graph on the planar domain. In the planar domain, geodesic curves are defined by line segments whose counterparts on $\mathcal{M}$, with respect to a diffeomorphism $\phi : \mathcal{M} \to \mathbb{R}^2$, are smooth approximations of geodesic paths. Our method defines a family of cut-graphs of $\mathcal{M}$ which can target different applications, such as global parameterization with respect to different criteria (*e.g.*, minimal length, minimization of the parameterization distortion, or interpolation of points as required by remeshing and texture mapping) or the calculation of polygonal schemes for surface classification. The proposed approach finds a cut-graph of an arbitrary triangle mesh $\mathcal{M}$ with n vertices and b boundary components in $O((b-1)n)$ time if $\mathcal{M}$ has 0-genus, and $O(n(\log(n)+2g+b-1))$ time if $g \geq 1$. The associated polygonal schema is reduced if $g = 0$, and it has a constant number of redundant edges otherwise.

1 Introduction

During the last years, the global parameterization of arbitrary 2-manifold triangle meshes has gained an increasing attention due to the impact on several research problems: its theoretical aspects are related to the surface classification and the computation of a global embedding enables to apply standard approximation techniques (*i.e.*, remeshing and polynomial approximation), texture mapping, and compression.

[1] Istituto di Matematica Applicata e Tecnologie Informatiche
Consiglio Nazionale delle Ricerche, Genova
Via De Marini 6, 16149 Genova, Italy
e-mail: *{patane,spagnuolo,falcidieno}@ge.imati.cnr.it*

Preprint submitted to Elsevier Science *29 September 2006*

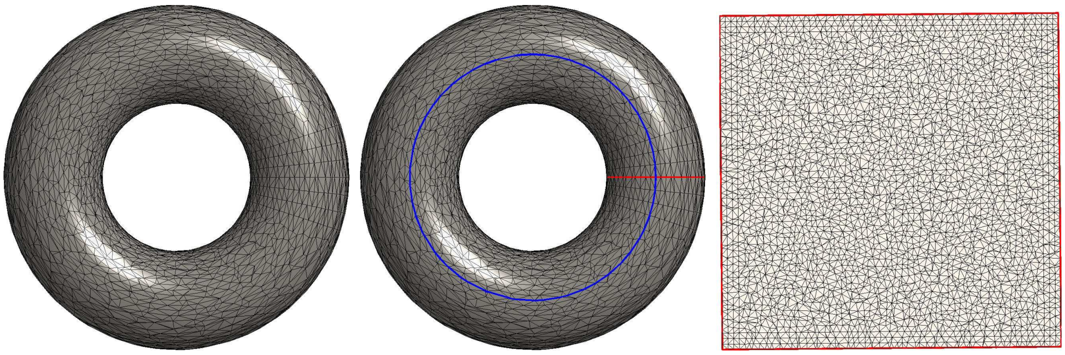

(a) (b) (c)

Fig. 1. (a) Input surface with genus one, (b) cut-graph with a meridian loop (red curve) and a longitude cut (blue curve), (c) shape-preserving parameterization on the unit square.

First of all, let us introduce some basic notations and formally define the global parameterization problem. We represent a compact and connected surface as a triangle mesh $\mathcal{M} := (M,T)$ where $M := \{\mathbf{p}_i,\, i = 1,\dots,n\}$ is a set of n vertices and T is an *abstract simplicial complex* which defines the adjacency among the vertices. If $\mathcal{M}$ has e edges, f faces, and b boundary components, $\chi(\mathcal{M}) := n-e+f$ is called the *Euler characteristic* and it is related to the genus g of $\mathcal{M}$ by the relation $g = \frac{1}{2}(2-\chi(\mathcal{M})-b)$. The *global parameterization* problem consists of finding a simplicial isomorphism $\varphi : \mathcal{M} \to \mathcal{P} \subseteq \mathbb{R}^2$, with $\mathcal{P}$ parameterization domain, that is, an injective map

$$\varphi|_M : M \to \Omega \subseteq \mathbb{R}^2$$
$$\mathbf{p}_i \mapsto \mathbf{t}_i$$

with $\Omega := \{\mathbf{t}_i,\, i = 1,\dots,n\}$ and such that $\mathcal{P} := (\Omega,T)$ is a planar disc [2] isomorphic to $\mathcal{M}$. The map φ is extended from the vertices M to the surface $\mathcal{M}$ by using barycentric coordinates.

Obviously, if $\mathcal{M}$ has genus $g \geq 1$, or at least two boundary components, it is necessary to cut $\mathcal{M}$ along a path γ, called the *cut-graph*, in order to unfold $\mathcal{M}$ onto $\mathcal{P}$. As shown in Fig. 1, a torus can be represented as a square with opposite edges identified; we note that all four vertices of the square are mapped to a single point on the corresponding surface. Then, we associate to each surface or patch of genus one, called *topological handle*, a *meridian* (resp., *longitude*) cut which is around (resp., along) the handle. Let us suppose that each closed curve γ on $\mathcal{M}$ has an anticlockwise orientation; γ^{-1} means that we have reversed the ordering of its vertices. Labeling the meridian and longitude cut as γ_1 and γ_2 respectively, we can represent the torus by a 4-sided polygon whose edges are identified according to the symbols $\gamma_1\beta_1\gamma_1^{-1}\beta_1^{-1}$. In the general case, the cut of $\mathcal{M}$ along γ defines the disc-like surface

[2] $\mathcal{P}$ is called *disc* or *disc-like surface* if it has 0-genus and one boundary component.

$\overline{\mathcal{M}} := (\mathcal{M} - \gamma)$ which is homeomorphic to a simple polygon $\mathcal{P}$, and by the identification of the edges of $\partial\mathcal{P}$ we get back the input surface. The polygon $\mathcal{P}$, together with the identification of its boundary edges, is called a *polygonal schema* of $\mathcal{M}$ and the following ones have a theoretical importance for surface classification and Computer Graphics applications:

- *polygonal schema of minimal length*: γ has minimal length;
- *reduced polygonal schema*: γ is a *fundamental system of loops with base point* $\mathbf{s} \in \mathcal{M}$, that is, a set of closed, simple, and pair-wise disjoint paths which share $\mathbf{s}$;
- *canonical polygonal schema*: the evaluation of the polygonal schema of the torus can be generalized to the case of a surface of genus g with b boundary components $\{\alpha_1, \dots, \alpha_b\}$ and it brings to a $(4g+3b)$-sided polygon of the form (Massey, 1967)

$$\gamma_1\beta_1\gamma_1^{-1}\beta_1^{-1}\dots\gamma_g\beta_g\gamma_g^{-1}\beta_g^{-1}\Gamma_1\alpha_1\Gamma_1^{-1}\dots\Gamma_b\alpha_b\Gamma_b^{-1}. \tag{1}$$

  In this case, the i-th handle is identified by $\gamma_i\beta_i\gamma_i^{-1}\beta_i^{-1}$ and each boundary component α_i is reached by a *link path* Γ_i, $i = 1, \dots, b$. The polygonal schema of the sphere is $\gamma_1\gamma_1^{-1}$.

Related work. Arbitrary cut-graphs can be found in $O(gn)$ time and paths interpolating a common base point can be optimized in polynomial time (De Verdiere and Lazarus, 2002). Finding the cut of minimal length is NP-hard (Erickson and Har-Peled, 2002), but any given cut can be converted to a $O(\log^2(g))$-approximation of the minimum cut-graph, which is neither reduced nor canonical, in $O(g^2 n \log(n))$ time. In (Erickson and Whittlesey, 2005), the shortest set of loops of the fundamental group is evaluated in $O(n\log(n))$ time by using the Dijkstra's shortest path algorithm (Dijkstra, 1959) and the method applies to closed and analytic Riemannian 2-manifolds.

In (Steiner and Fischer, 2002b), the cut-graph γ of a closed surface $\mathcal{M}$ is built as the minimum spanning tree (Kruskal, 1956) of the $2g$ boundaries generated by duplicating the g longitudes found by using the EdgeBreaker algorithm (Lopes et al., 2002), which moves a contour σ on $\mathcal{M}$ while maintaining it homotopic to a circle. For surfaces with boundary, longitudes cannot be extracted because boundary components prevent to sweep σ on $\mathcal{M}$ in a homotopic way. A specialization of this method for texture mapping on closed surfaces of genus one has been proposed in (Steiner and Fischer, 2004).

In (Gu et al., 2002), the cut-graph γ is built by using an iterative procedure. At first, a seed triangle is removed from $\mathcal{M}$ and its boundary is marked as active; at each step, one triangle adjacent to the current boundary is removed while maintaining the set of removed faces homeomorphic to a disc. The visiting process is performed by considering at first those faces which are closest to the seed and iterating this step until all the triangles have been visited. The boundary of the region gives the cut-graph. Since this procedure depends on the triangle mesh connectivity, a post-processing based on the Dijkstra's algorithm is used to make γ shorter and smoother.

Several methods in Computer Graphics use the Reeb graph for solving topological problems, such as the work presented in (Ni et al., 2004; Patanè et al., 2004; Steiner and Fischer, 2002a) that is closely related to our method. In (Patanè et al., 2004), the Reeb graph is used to compute a decomposition of arbitrary shapes into 0-genus charts and it is applied to local parameterization and texture mapping (Zhang et al., 2005). In this paper, we exploit the Morse theory to search a family of cut-graphs for the global parameterization problem; furthermore, we generalize and increase the flexibility of the procedure used in (Patanè et al., 2004) for finding the cut-graphs of 0-genus patches. In (Steiner and Fischer, 2002a), the cut-graph is a tree defined by the iso-contours of the geodesic distance from a source point and connected by using a geodesic-based procedure.

In (Ni et al., 2004), a harmonic scalar field f is achieved by solving the equation $\Delta f = 0$, where Δ is the Laplace-Beltrami operator, subject to the Dirichlet boundary conditions $\mathcal{B} := \{f(\mathbf{p}_i) = a_i,\ i \in \mathcal{C} \subseteq \{1,\dots,n\}\}$. For piecewise linear functions on triangulated surfaces, the discrete Laplacian operator is defined as

$$\Delta f(\mathbf{p}_i) = \sum_{j \in N(i)} w_{ij}(f(\mathbf{p}_j) - f(\mathbf{p}_i)),$$

where $N(i)$ is the set of vertices adjacent to the vertex i and w_{ij} is the weight associated to the directed edge (i,j). In (Pinkall and Polthier, 1993), the discrete harmonic weights are chosen as $w_{ij} := 1/2(\cot\alpha_{ij} + \cot\beta_{ij})$, where α_{ij} and β_{ij} are the angles opposite to the edge (i,j). The harmonicity of the (discrete) scalar field f is equivalent to the linear system $\mathbf{L}\mathbf{f}^{\star} = \mathbf{b}$, where $\mathbf{f}^{\star} := (f(\mathbf{p}_i))_{i \in \{1,\dots,n\} \setminus \mathcal{C}}$ is the vector of unknowns, $\mathbf{b}$ is a constant vector related to the boundary conditions $\mathcal{B}$, and $\mathbf{L}$ is the *Laplacian matrix*

$$\mathbf{L}_{ij} := \begin{cases} \sum_{k \in N(i)} w_{ik} & \text{if } i = j, \\ -w_{ij} & \text{if } (i,j) \text{ is an edge of } \mathcal{M}, \\ 0 & \text{otherwise.} \end{cases} \tag{2}$$

Since the selection of the constrained vertices $\{\mathbf{p}_i,\ i \in \mathcal{C}\}$ is left to the user, a different choice of $\mathcal{C}$ gives a different f; for instance, the harmonic fields shown in Fig. 4(c-d) have been achieved by choosing 1 maximum (red point) and 1 minimum (blue point). The construction of harmonic scalar fields is used in (Ni et al., 2004) to build a cut-graph which interpolates a set of critical points whose maxima and minima are selected by the user among the vertices of $\mathcal{M}$. Furthermore, it

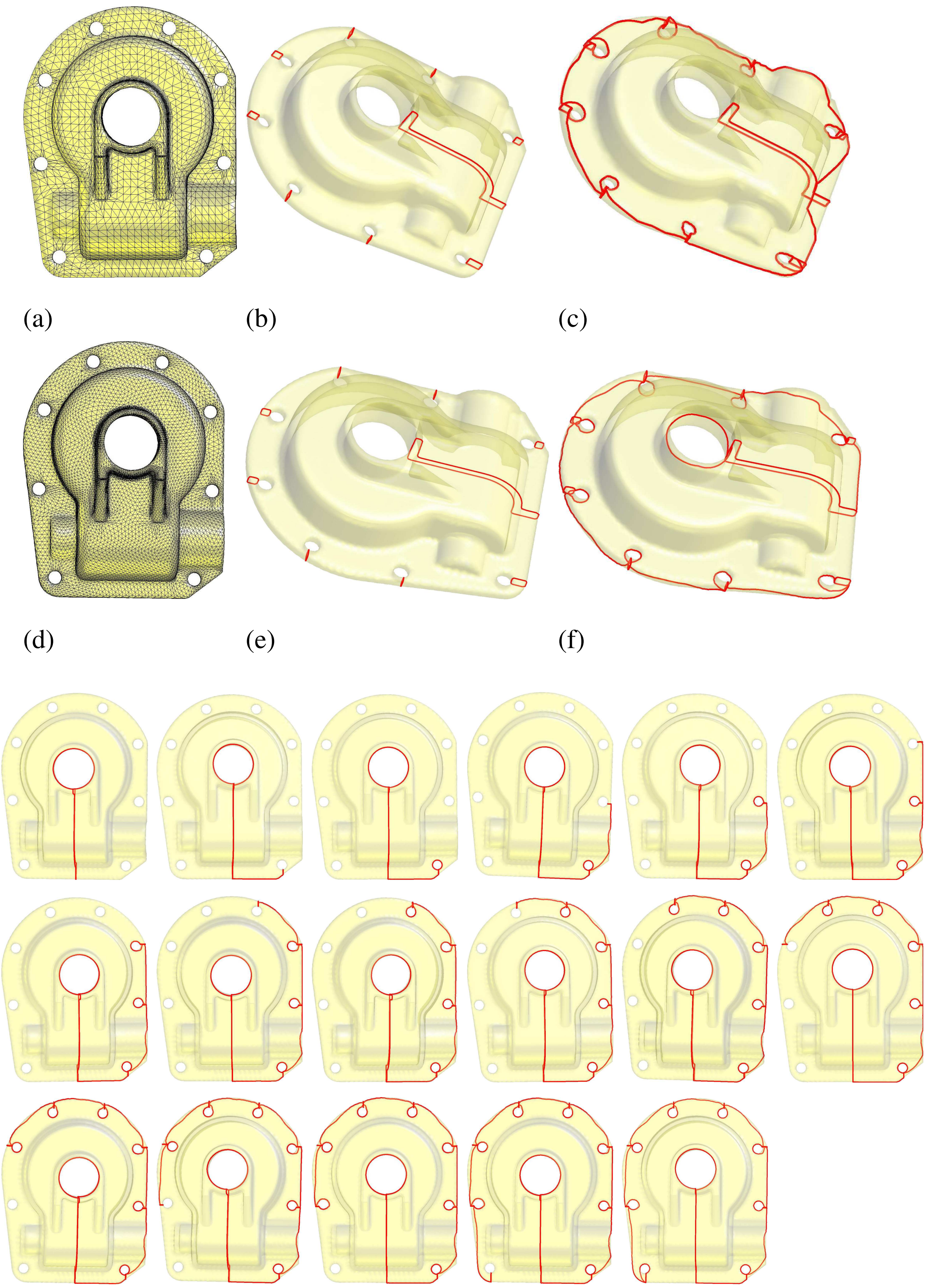

Fig. 2. (a, d) Coarse and refined triangle mesh of genus nine, (b, e) meridian loops, (c, f) cut-graphs. Steps of the iterative procedure which converts the surface (b) of 0-genus with eighteen boundary components into a disc-like surface while building its cut-graph.

is possible to define harmonic fields of closed surfaces with a minimal number of critical points (*i.e.*, 1 maximum, 1 minimum, and $2g$ saddles). Dealing with open surfaces instead of closed 2-manifolds arises additional saddles (see Proposition 1) which create a redundancy of the number of branchings of the cut-graph and possible ambiguities in tracing flow-lines.

The degree of freedom for the selection of the cut-graphs decreases if we search for the reduced polygonal schema or the homology base of $\mathcal{M}$ (Massey, 1967), which are commonly used for surface classification and global *conformal* parameterization, that is, a mapping φ which preserves the angles (Gu and Yau, 2003). The evaluation of the canonical polygonal schema requires to link the cut loops of the topological handles and the boundary components of $\mathcal{M}$ with a minimal number of paths. However, any polygonal schema can be converted to the canonical form with a set of reduction operations whose computational cost for a closed surface is $O(t\log(t))$, with t total number of vertices, edges, and faces (Vegter and Yap, 1990).

Overview and contributions. Our approach to the global parameterization problem consists of two steps: (a) identification and cut of the topological handles of $\mathcal{M}$ along the iso-contours $\Gamma := \{\gamma_i\}_i$ of a scalar field f on $\mathcal{M}$, and (b) construction of a family of cut-graphs which include Γ. An overview of the method is given in Fig. 2 and 3. Previous work on the cut-graph search assumes to deal with closed or Riemannian surfaces as in (Erickson and Whittlesey, 2005; Ni et al., 2004; Steiner and Fischer, 2002a), does not define smooth cut-graphs which approximate the geodesics, and the cut-graphs defined in (Ni et al., 2004) do not include meridian loops or constraints on the length, regularity, and shape (see Section 2 and 3). These elements are the starting point of our framework, whose main features with respect to the state of the art are:

- *flexibility*: our method does not define a single cut-graph but it builds a *family* of cut-graphs $\mathcal{F}$. Once we have built the Reeb graph and the Laplacian matrix of $\mathcal{M}$, each cut-graph is calculated in linear time. The cut-graph γ which converts $\mathcal{M}$ to a disc-like surface $\overline{\mathcal{M}}$ enables to parameterize $\overline{\mathcal{M}}$ with any of the standard techniques (Floater and Hormann, 2005; Sheffer et al., 2005; Zayer et al., 2005). Then, in $\mathcal{F}$ we select those that satisfy constraints such as smoothness degree, minimal length and parameterization distortion;
- *generality* and *openness*: closed and bordered surfaces are treated with a unique approach. Furthermore, the method proposed for joining the cut loops of the topological handles of $\mathcal{M}$ does not rely on the fact that they are meridians or longitudes, nor does it depend on the specific methods that are used for their identification;
- *smoothness* and *"independence" of the mesh connectivity*: the cut-graph is not affected by the mesh connectivity. If harmonic weights (Pinkall and Polthier, 1993) are chosen, the cut-graph is an approximation of a curve of class C^s, $s \geq 2$,

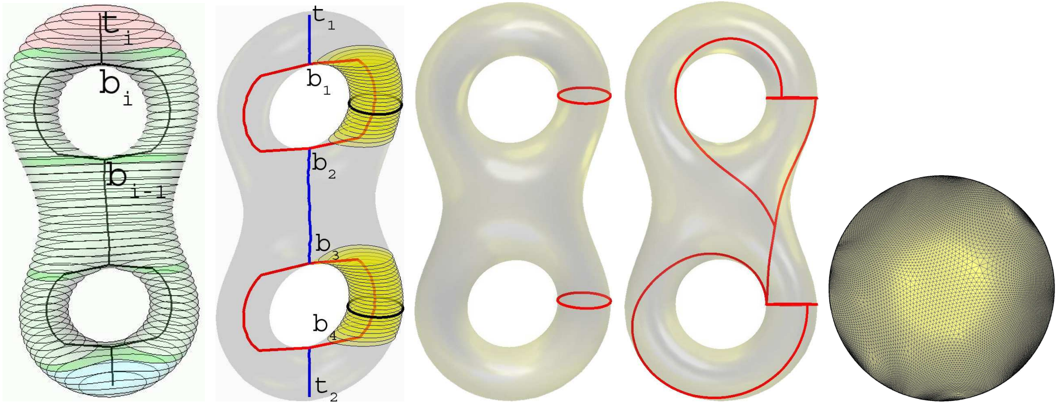

(a) (b) (c) (d) (e)

Fig. 3. (a) The Reeb graph with respect to the height function, (b) the node classification and meridian loops, (c) the 0-genus surface with four boundary components achieved by cutting the topological handles along the black iso-contours shown in (b), (d) the cut-graph, and (e) the shape-preserving parameterization on the unit circle (Floater, 1997).

everywhere with the exception of few points where a C^0-regularity holds. On the contrary, previous work guarantees a C^0-smoothness because it is based on mesh traversal techniques such as the Dijkstra's algorithm and the minimum spanning tree;

- *computational cost*: the cut-graph is computed in $O((b-1)n)$ time if $g=0$ and $O(n(\log(n)+2g+b-1))$ time if the input surface has genus $g \geq 1$. Finally, each new cut-graph is calculated in $O((2g+b-1)n)$ time and it defines a reduced polygonal schema or with $2g$ redundant edges.

The paper is organized as follows: Section 2 introduces the core of our method, in Section 3 we discuss its properties, degrees of freedom, and limitations. Finally, future work concludes the paper.

2 Cutting surfaces of arbitrary genus

We approach the search of a family of cut-graphs by reducing it to the following sub-problems (see Fig. 3):

(1) locate the g topological handles of $\mathcal{M}$ and cut each of them along one of its meridian loops by duplicating it into two identical loops (see Section 2.1). Therefore, $\mathcal{M}$ is converted into a 0-genus surface $\mathcal{M}^\star$ with $2g+b$ boundary components;
(2) join the $2g+b$ boundary components in order to convert $\mathcal{M}^\star$ to a new surface $\overline{\mathcal{M}}$ with 0-genus and a unique boundary γ (see Section 2.2). Then, the polyg-

onal schema of $\overline{\mathcal{M}}$ is calculated and the surface is unfolded by applying any parameterization of disc-like surfaces.

The degrees of freedom in the selection of the the meridian loops and in the joining procedure generate a *family of cut-graphs*.

2.1 Locating and cutting topological handles

The genus of $\mathcal{M}$, which is computed in linear time through the Euler formula, is the maximum number of disjoint and non-separating *loops* $\gamma_1,\ldots,\gamma_g$ on $\mathcal{M}$; that is, the set of closed curves such that $\gamma_i \cap \gamma_j = \emptyset$, $i \neq j$, and $\mathcal{M} - (\gamma_1 \cup \ldots \cup \gamma_g)$ is a connected 0-genus surface. Since the Euler formula does not give information for locating and cutting the g topological handles, our approach builds on the Reeb graph theory (Reeb, 1946), which can be used to code $\mathcal{M}$ in a combinatorial structure whose cycles identify its handles and whose associated iso-contours locate the meridian curves along which the surface has to be cut. The Reeb graph is formally defined as follows (Reeb, 1946).

Definition 1 *Let $\mathcal{M}$ be a compact manifold and $f : \mathcal{M} \rightarrow \mathbb{R}$ be a continuous function. The* Reeb graph R_G *of $\mathcal{M}$ with respect to f is the quotient space of $\mathcal{M} \times \mathbb{R}$ defined by the relation* " $\sim$ " *with*

$$(\mathbf{p}, f(\mathbf{p})) \sim (\mathbf{q}, f(\mathbf{q})) \leftrightarrow f(\mathbf{p}) = f(\mathbf{q})$$

and $\mathbf{p}$, $\mathbf{q}$ *belong to the same connected component of $f^{-1}(f(\mathbf{p}))$.*

The Reeb graph of $\mathcal{M}$ with respect to f is obtained by contracting to points the connected components of the level sets of f. For 2-manifold surfaces and Morse mapping functions, several interesting results hold. Given a C^2 function $f : \mathcal{M} \rightarrow \mathbb{R}$, the *critical points* of f are defined as those points $\mathbf{p} \in \mathcal{M}$ such that $\nabla f(\mathbf{p}) = \mathbf{0}$ and they correspond to maxima, minima, and saddles. The function f is *Morse* if all its critical points are *Morse*, that is, the Hessian matrix of f in $\mathbf{p}$ is not singular. In this case, we have that branchings in the Reeb graph can occur only in correspondence of the level sets that go through the saddle points of f. For a closed surface $\mathcal{M}$, the relation between the critical points of $(\mathcal{M}, f)$ and $\chi(\mathcal{M})$ (or equivalently g) is given by the condition (Banchoff, 1967; Milnor, 1963):

$$\chi(\mathcal{M}) = \text{minima} - \text{saddles} + \text{maxima}.$$

The following result provides the link between the topology of a closed or bordered surface $\mathcal{M}$ and its Reeb graph (Cole-McLaughlin et al., 2003).

Proposition 1 *Let $\mathcal{M}$ be a connected, orientable 2-manifold of genus g, $f : \mathcal{M} \rightarrow \mathbb{R}$ a Morse function, and R_G the Reeb graph of $\mathcal{M}$ with respect to f. Then,*

(a) Dist. Baryc. (b) Int. Geod. Dist. (c) Harm. Field (d) Harm. Field

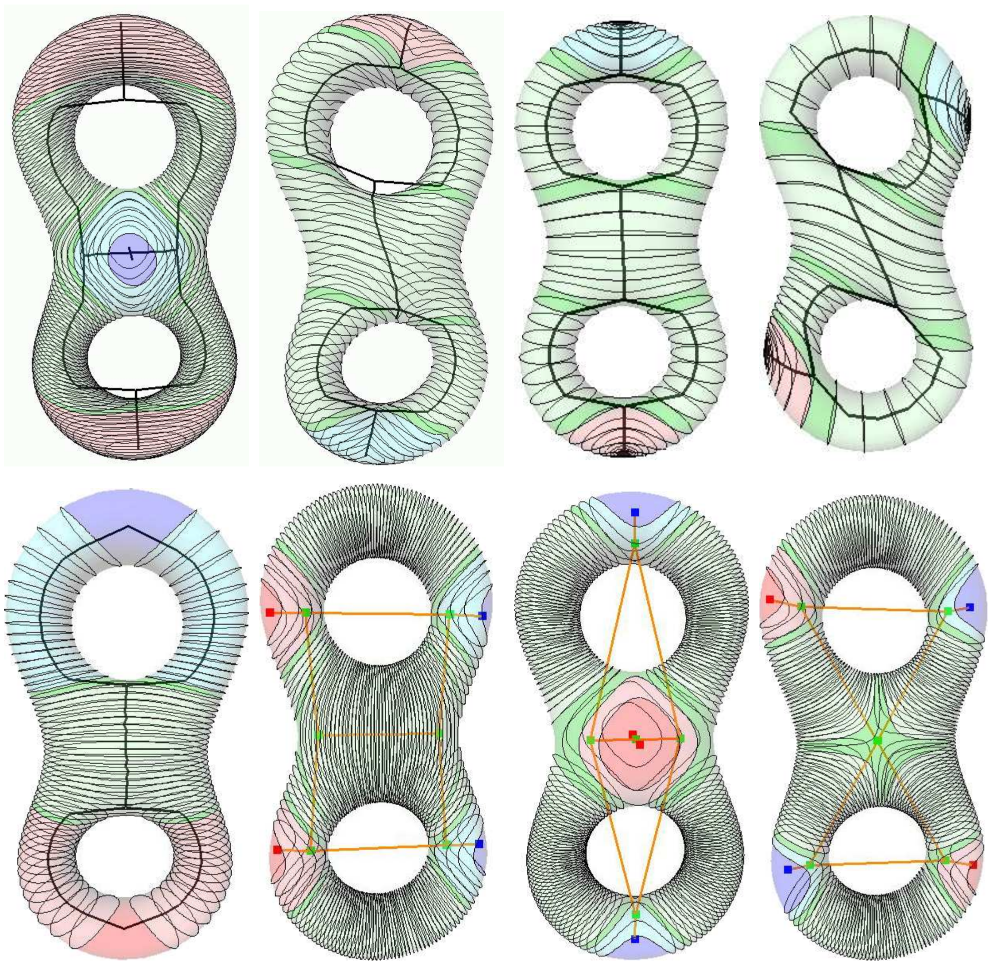

(e) 2^{th} Eigenfun. (f) 3^{th} Eigenfun. (g) 4^{th} Eigenfun. (h) 5^{th} Eigenfun.

Fig. 4. Iso-contours, critical regions, and Reeb graph (Biasotti, 2004; Lazarus and Verroust, 1999) of the bi-torus with respect to several mapping functions. Red regions (resp., blue and green) include maxima (resp., minima and saddles) of the scalar field. The harmonic scalar fields shown in (c-d) have been achieved by using as maximum and minimum the red and blue vertex pointed by the incident arc of the Reeb graph.

- *if $\mathcal{M}$ is closed, R_G has g loops;*
- *if $\mathcal{M}$ has $b \geq 1$ boundary components, R_G has k loops with $g \leq k \leq 2g+b-1$.*

Proposition 1 guarantees that if $\mathcal{M}$ is a closed surface the number of loops in the Reeb graph does not depend on the choice of f. If we consider a surface with boundary some cycles of R_G may not be related to the topological handles of $\mathcal{M}$; therefore, they are *spurious cycles* due to the boundary components.

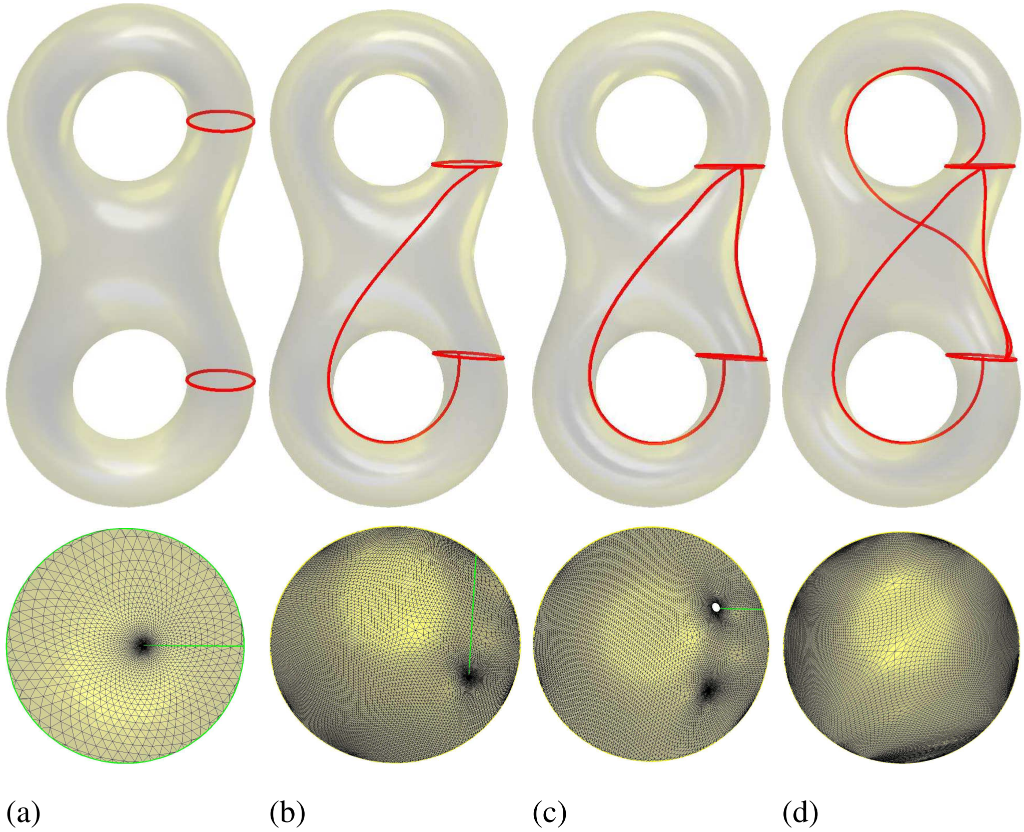

Fig. 5. Iterative procedure used to build the cut-graph of the bitorus (f is the height function); each (green) line-segment on the unit disc identifies a link-path of the final cut-graph. After three steps the input 0-genus surface with four boundary components in (a) is converted into a disc-like surface shown in (d).

Analogous definitions and properties apply in the discrete setting (Biasotti, 2004; Carr et al., 2003; Lazarus and Verroust, 1999; Pascucci and Cole-McLaughlin, 2002; Wood et al., 2004) where f is defined on the edges and faces of $\mathcal{M}$ by linearly interpolating the values $\{f(\mathbf{p}_i)\}_{i=1,\ldots,n}$. Common choices for f are the height function (Reeb, 1946), the integral geodesic distance (Hilaga et al., 2001), the geodesic distance from curvature extrema (Mortara and Patanè, 2002), harmonic scalar fields (Ni et al., 2004), and the eigenfunctions of the Laplacian matrix of $\mathcal{M}$ (Dong et al., 2006) (see Fig. 4).

In our work, we use the discretization framework defined in (Biasotti, 2004), where the Reeb graph is extracted by a uniform slicing of the triangle mesh under the mapping of a continuous function which admits degenerate critical points. More precisely, this method uses a discretization of the range of f and codes the evolution of the level set components $f^{-1}(\alpha_i)$ computed at a finite set of values $\alpha_i \in \mathbb{R}$. Each connected component of the iso-contours $f^{-1}(\alpha_i)$ is represented by a node i of R_G; the node degree d_i is defined as the number of edges incident to i in R_G and a node i is classified as *terminal* if $d_i = 1$, as *internal* if $d_i = 2$, and as *branching*

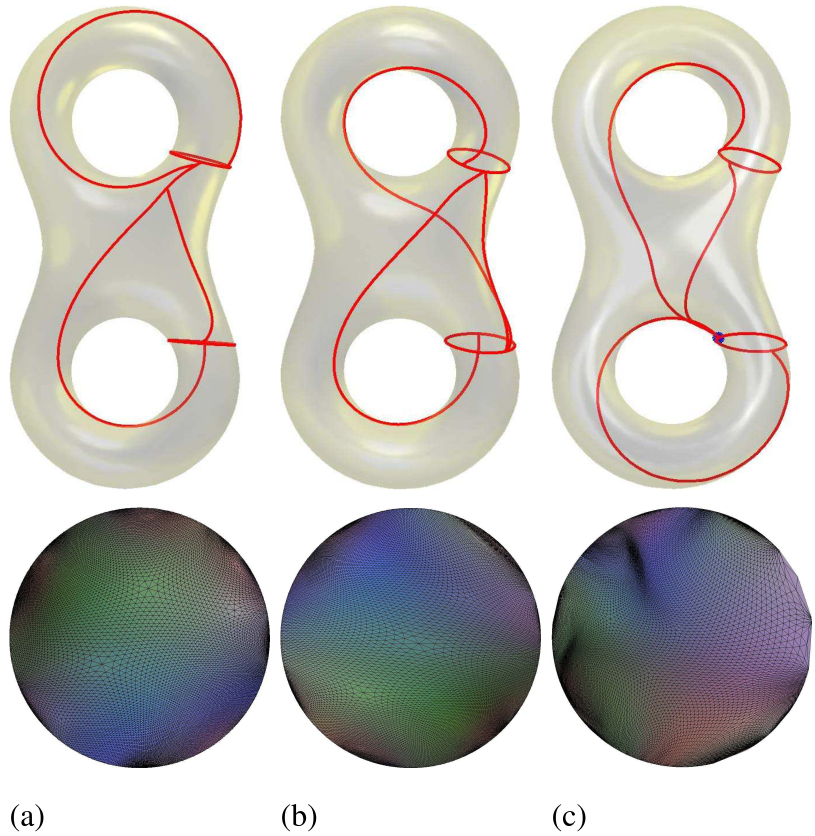

Fig. 6. Cut-graphs of the bitorus; each column shows the cut and the corresponding shape-preserving parameterization. (a) Bifurcations are admitted ($|\gamma| = 19.7$, $L^2(\mathcal{M}) = 13$), (b) bifurcations are discarded ($|\gamma| = 19.06$, $L^2(\mathcal{M}) = 20.8$), (c) a given source point is interpolated ($|\gamma| = 23.74$, $L^2(\mathcal{M}) = 59.9$).

if $d_i \geq 3$. The holes of $\mathcal{M}$ possibly contained within two consecutive iso-contours are easily detected by using the Euler formula in the strips of triangles. This simple procedure is used to locally check and update the discretization of the Reeb graph while keeping its topological correctness, as stated by Proposition 1. Given a mapping function f on $\mathcal{M}$, the construction of the Reeb graph R_G has a computational cost which is the maximum between $n\log(n)$ and $n+m$, where m is the number of vertices inserted by the slicing process. Therefore, in the average case we have that $m << n$ and the construction of the Reeb Graph requires $O(n\log(n))$ time; details concerning the method to extract and code R_G can be found in (Biasotti, 2004).

We now describe how the topological handles of $\mathcal{M}$ are identified and cut without disconnecting the input surface, while reducing its genus to zero (see Fig. 3(a-b)). Starting from a branching node $b := b_i$ of R_G we walk on one of its branches along a path $\mathcal{H}$ of internal nodes until a terminal or a new branching node occurs. Let $\mathcal{M}_{\mathcal{H}}$ be the open region of $\mathcal{M}$ delimited by $\mathcal{H}$, that is, the open sub-mesh delimited by the iso-contours associated to b and q, with q last node of $\mathcal{H}$. If $q := t_i$ is a terminal node, $\mathcal{M}_{\mathcal{H}}$ has 0-genus (Milnor, 1963); therefore, cuts will not be performed. Otherwise, $q := b_{i-1}$ is a branching node and we have to decide if $\mathcal{M}_{\mathcal{H}}$

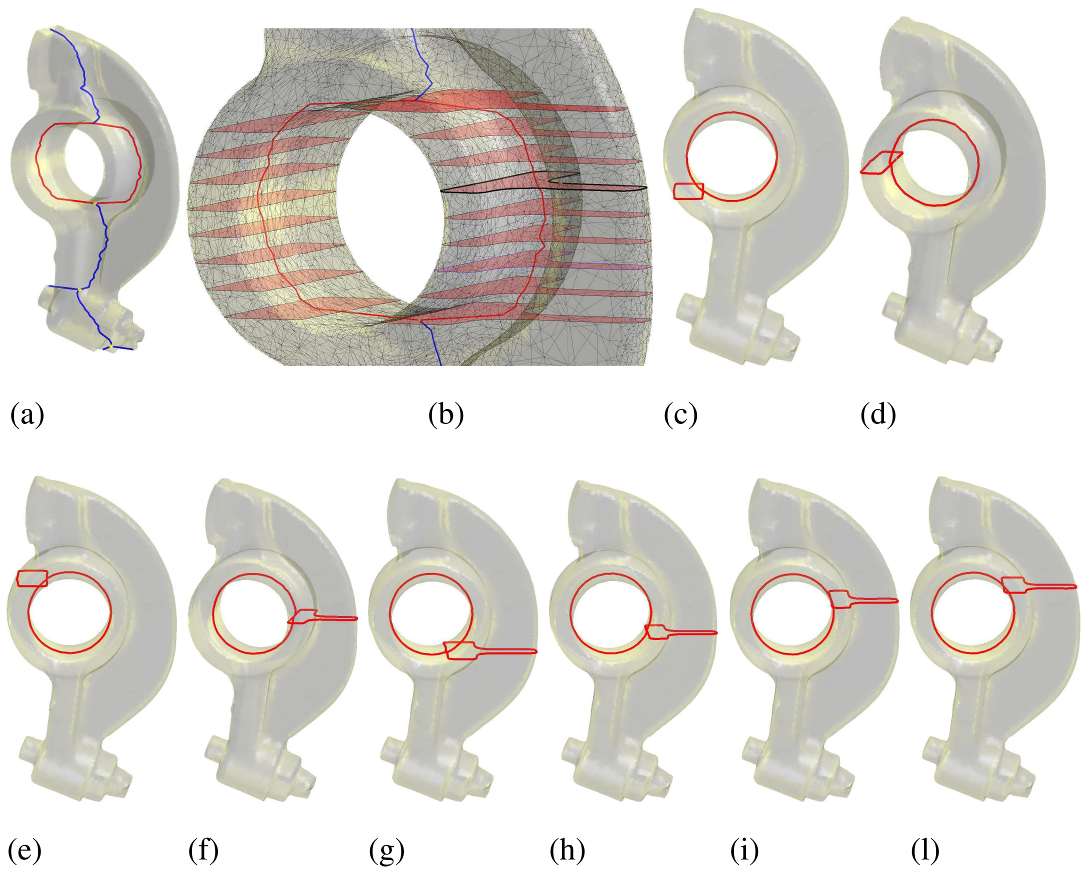

Fig. 7. (a) The Reeb graph with respect to the height function, (b) loop identification (red curve) and related iso-contours, (c-l) family of cut-graphs $\mathcal{F}$ defined by the different iso–contours shown in (b). In $\mathcal{F}$, (c) is the cut-graph of shortest length and (l) is the one which induces the minimal L^2-stretch with respect to the shape-preserving parameterization.

is part of a topological handle. This check is done by considering the genus $\overline{g}$ of $\mathcal{M}$ after the cut: if the cut does not disconnet $\mathcal{M}$ and $\overline{g} = (g-1)$, then $\mathcal{M}_{\mathcal{H}}$ is sliced along a meridian loop associated to any suitable internal node of $\mathcal{H}$. The meridian loop of minimal length or the one associated to the node which is in the middle of $\mathcal{H}$ are possible choices. Otherwise, the handle cut is discarded. Then, the nodes of $\mathcal{H}$ are marked as visited and the next iterations consider all the other paths that emanate from b_{i-1} and not analyzed yet. The algorithm proceeds on the non-visited arcs of R_G until g cuts have been performed; therefore, the stop can happen before visiting the whole graph and the computational cost of the loop search is linear in the number of nodes of R_G.

With reference to Fig. 3(b), starting from the branching node b_1 we walk on the arc of the Reeb graph until the terminal node t_1 is reached; the corresponding surface patch does not identify a topological handle of the bitorus and cuts will not be done. Then, we move from b_1 to b_2 along the arc on the right side and we perform a cut along one of the shown iso-contours thus reducing the genus to one and generating

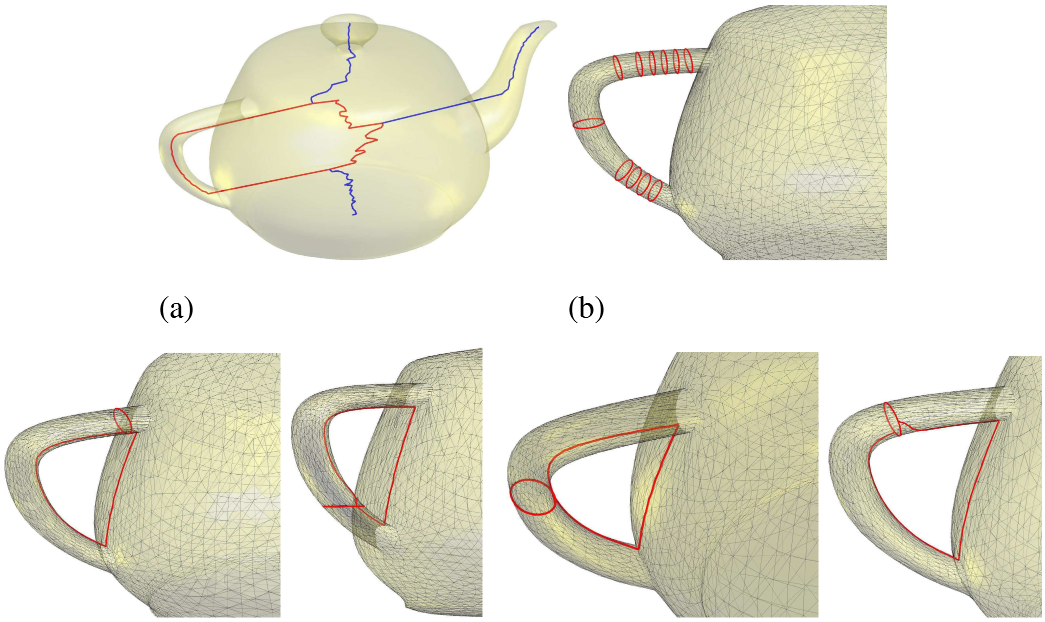

$|\gamma| = 13.21$ $L^2(\mathcal{M}) = 48.23$ | $|\gamma| = 14.83$ $L^2(\mathcal{M}) = 43.15$ | $|\gamma| = 15.26$ $L^2(\mathcal{M}) = 40.11$ | $|\gamma| = 14.16$ $L^2(\mathcal{M}) = 44.01$

Fig. 8. First row: (a) the Reeb graph with respect to the geodesic distance, (b) the meridian loops of the topological handle used to build the family of cut-graphs. Second row: four cut-graphs and information regarding their length and L^2-stretch with respect to the shape-preserving parameterization.

two boundary components. Let us now suppose that the algorithm visits the graph arc from b_2 to b_1 on the left; in this case, each iso-contour disconnects the surface and therefore will be discarded. The same discussion applies to the surface patch identified by the arc from b_2 to b_3; finally, a cut is performed along the arc b_3b_4. Since $g = 2$, the algorithm stops and the output is a surface of 0-genus with four boundary components (see Fig. 3(c)). The next section discusses how these handle loops are converted to a cut-graph through an iterative procedure (see Fig. 3(d-e)).

2.2 Cut-graph construction and polygonal schema evaluation

Once $\mathcal{M}$ has been reduced to a 0-genus surface $\mathcal{M}^\star$ with $\bar{b} := (2g + b)$ boundary components $\{\gamma_i\}_{i=1,\dots,\bar{b}}$, we evaluate its cut-graph γ and the associated polygonal schema. Searching and optimizing a cut on a disc-like surface $\mathcal{S}$ through the correspondence between $\mathcal{S}$ and its parameterization domain were firstly proposed in (Gu et al., 2002). Here, an iterative procedure augments an initial coarse cut with a path which joins it to a sub-region with high L^2-stretch until the distortion is below a given threshold. The computational cost after k iterations is $O(kn\log(n))$ with n number of input vertices. In a similar way (see Fig. 5), we extend the method proposed in (Patanè et al., 2004) to join the boundary components on $\mathcal{M}^\star$ and we

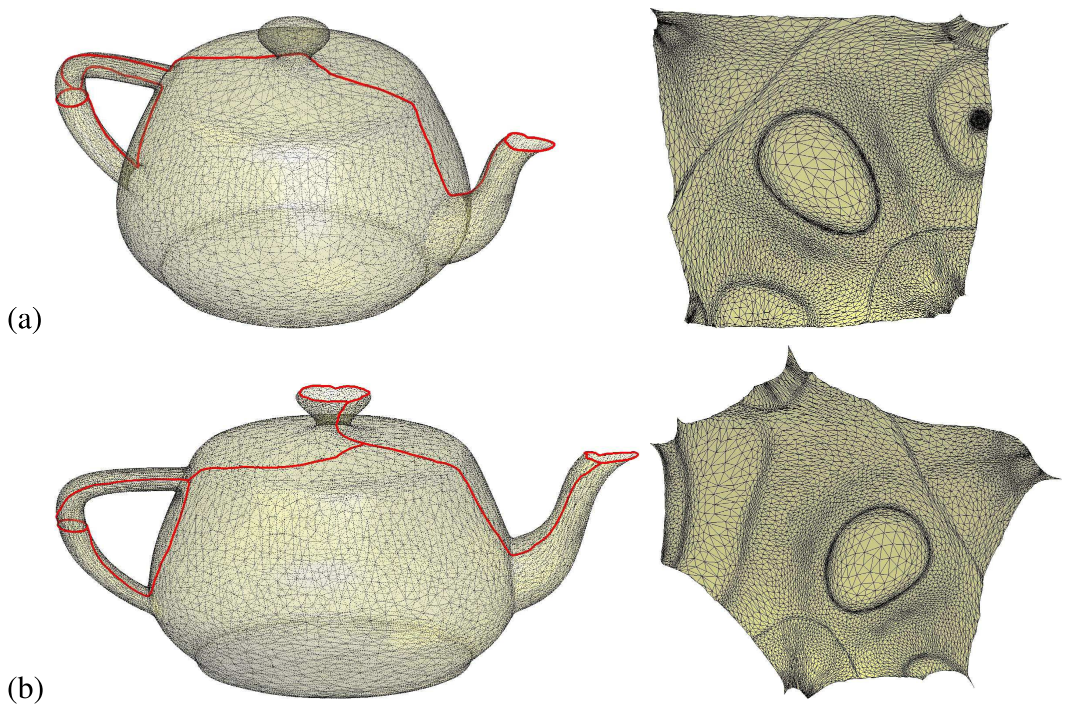

Fig. 9. The cut-graph and quasi-harmonic parameterization (Zayer et al., 2005) on a surface of genus-1 with (a) one and (b) two boundary components.

provide a greater flexibility for the cut selection and a lower computational cost.

Chosen one boundary component γ_1 (for example, the longest one), we parameterize $\mathcal{M}$ with respect to γ_1 by using the barycentric coordinates method (Floater, 1997) or the mean-value coordinates (Floater, 2003). This is equivalent to solve the linear system $\mathbf{L}_1\varphi_1 = \mathbf{b}_1$, where the matrix $\mathbf{L}_1$ is defined by the connectivity and geometry of $\mathcal{M}$ in a way similar to (2), and $\mathbf{b}_1$ forces γ_1 to be mapped on a convex planar curve (*e.g.*, the unit circle). Therefore, we define the isomorphism $\phi : \mathcal{M} \rightarrow \mathcal{D} := (\Omega^{'}, T)$ where $\Omega^{'} \subseteq \mathbb{R}^2$ is a planar domain with b convex loops $\{\beta_i := \phi(\gamma_i)\}_{i=1}^{b}$ (see Fig. 5(a)). At the first step, we consider the line segment $[\mathbf{p},\mathbf{q}]$ of minimal length which joins the external loop β_1 to its closest boundary component β_k with respect to the Euclidean distance in $\mathbb{R}^2$. The linear path $[\mathbf{p},\mathbf{q}]$ on the parameterization domain defines a curve, called *link path*, $\Gamma := \phi^{-1}([\mathbf{p},\mathbf{q}])$ on $\mathcal{M}$ that is used to convert the boundary components γ_1, $\gamma_k := \phi^{-1}(\beta_k)$ into a connected loop $\gamma := \{\gamma_1, \Gamma, \gamma_k^{-1}, \Gamma^{-1}\}$ (see Fig. 5(b)). This local cut defines a new surface $\overline{\mathcal{M}}$ with $(\bar{b}-1)$ boundary components instead of $\bar{b}$. By applying iteratively this process, after $(\bar{b}-1)$ steps we convert the loops $\{\gamma_i\}_{i=1,\dots,\bar{b}}$ to a connected cut γ on $\mathcal{M}$ (see Fig. 5(c-d)). This method can be used with any class of weights and our tests showed that smooth cut-graphs, which are approximations of the geodesic ones, are achieved with shape-preserving, harmonic, and mean-value weights. The only caution with harmonic weights is the possible creation of overlapping triangles; however, this situation did not happen in the tests of the paper. We note that

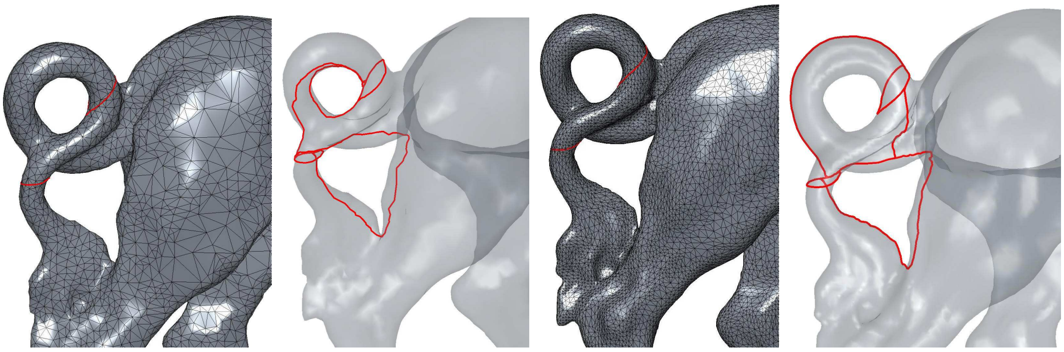

(a) (b)

Fig. 10. Influence of the mesh connectivity on the meridian loop selection and cut-graph extraction; f is the second eigenfunction of the Laplacian matrix of $\mathcal{M}$. Comparing (a) with (b) we note that a greater regularity of the mesh connectivity improves the quality of the upper part of the cut-graph which follows the high-curvature points of the handle. However, the handle cuts and the remaining part of the cut-graph show a similar shape.

γ depends mainly on the shape of β_1, β_k, and it is not affected by the quality of connectivity of $\mathcal{M}$ and the choice of the weights (see also Section 3).

At the i^{th}-step, the connectivity of the triangle mesh is updated only around the link path γ_i. Therefore, the Laplacian matrix $\mathbf{L}_{i+1}$ is achieved by locally updating $\mathbf{L}_i$ and adding the entries related to the new edges introduced by the cut γ_i, that is, the pairs $(\mathbf{p},\mathbf{q})$ that belong to the 1-stars intersected by γ_i. In this way, we efficiently transform $\mathbf{L}_i$ into $\mathbf{L}_{i+1}$ and we optimize the memory allocation for sparse matrices; the solution of the linear system, which defines ϕ, has to be recomputed by applying direct or iterative solvers of sparse linear systems (Golub and VanLoan, 1989). The insertion of γ in the triangulation might generate around γ triangles with small angles and edges; therefore, the corresponding entries of the coefficient matrix $\mathbf{L}_i$ might become unstable and arise an ill-conditioned linear system. A simple solution consists of identifying the geometric degeneracy in the triangles that we insert and associating them with constant weighs. In our tests, the use of irregularly sampled surfaces (*e.g.*, polygonized surfaces as shown in Fig. 17 and 18) did not arise these situations. The advantages of using cut-graphs which cut triangles instead of interpolating the edges of $\mathcal{M}$ are: the smoothness and stability of γ with respect to the surface sampling and connectivity, and a linear computational cost instead of $O(n\log(n))$. Finally, the points $\phi^{-1}(\mathbf{p})$, $\phi^{-1}(\mathbf{q})$ will appear as singularities of the cut-graph; in fact, they correspond to the spike points $\mathbf{p}$, $\mathbf{q}$ where the edge $[\mathbf{p},\mathbf{q}]$ intersects the boundary components which it joins.

We note that once we have built the Reeb graph and the Laplacian matrix of $\mathcal{M}$, each cut-graph is achieved in $O((2g+b-1)n)$ time; in fact, the handle iso-contours are stored during the construction of the Reeb graph and each iteration of the procedure requires only local updates of the coefficient matrix, a small storage over-

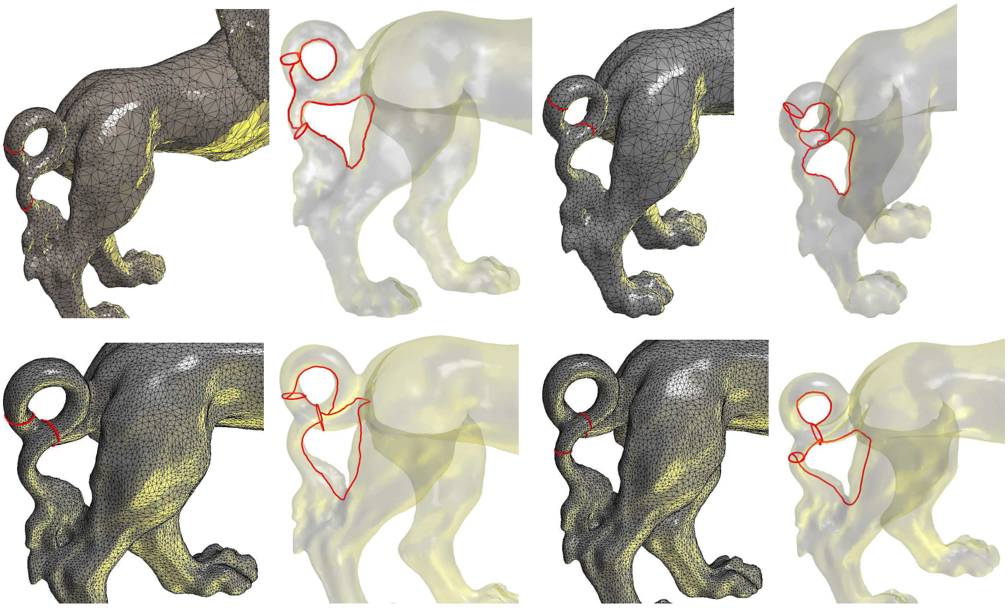

Fig. 11. Different choices of the meridian loops and related cut-graphs on a (first row) coarse and (second row) refined surface of genus two. In this example, f is the geodesic distance from curvature extrema.

head, and the solution of sparse linear systems. On the contrary, previous work (Steiner and Fischer, 2002a) requires to change the mapping function and to run the procedure which extracts the cut-graph, with a greater computational cost (*e.g.*, $O(n\log(n))$) and without degrees of flexibility. In the following, we discuss new options which can also be combined to define a *hybrid method*; the properties of γ and a comparison with previous work are discussed in Section 3.

Joining boundary components with or without bifurcations. If $\mathcal{M}$ has three or more boundary components, at a given iteration $k \geq 2$, the external boundary $\partial\mathcal{D}$ of the current parameter domain $\mathcal{D}$ includes the boundary components removed at the previous steps and the link paths which join them. Therefore, the line segment $[\mathbf{p},\mathbf{q}]$ of minimal length which links $\partial\mathcal{D}$ to its closest internal boundary component may have its origin $\mathbf{p}$ on an arc which corresponds to a link path Γ on $\mathcal{M}$; in this case, the point $\phi^{-1}(\mathbf{p}) \in \Gamma$ is a bifurcation of the cut (see Fig. 6(a)).

When we evaluate $[\mathbf{p},\mathbf{q}]$, we can restrict its search to the part of the external boundary which corresponds to the boundary components that were removed at the previous steps and neglecting the link paths which join them. Therefore, we constrain the cut to join the meridian loops and the boundary components without admitting bifurcations on the input surface (see Fig. 6(b)). In this case, we can suppose without loss of generality that the boundary component γ_i has been linked to γ_{i+1} by the link path Γ_i, with $i = 1,\dots,\bar{b}-1$. Since each cut Γ_i has an opposite counterpart

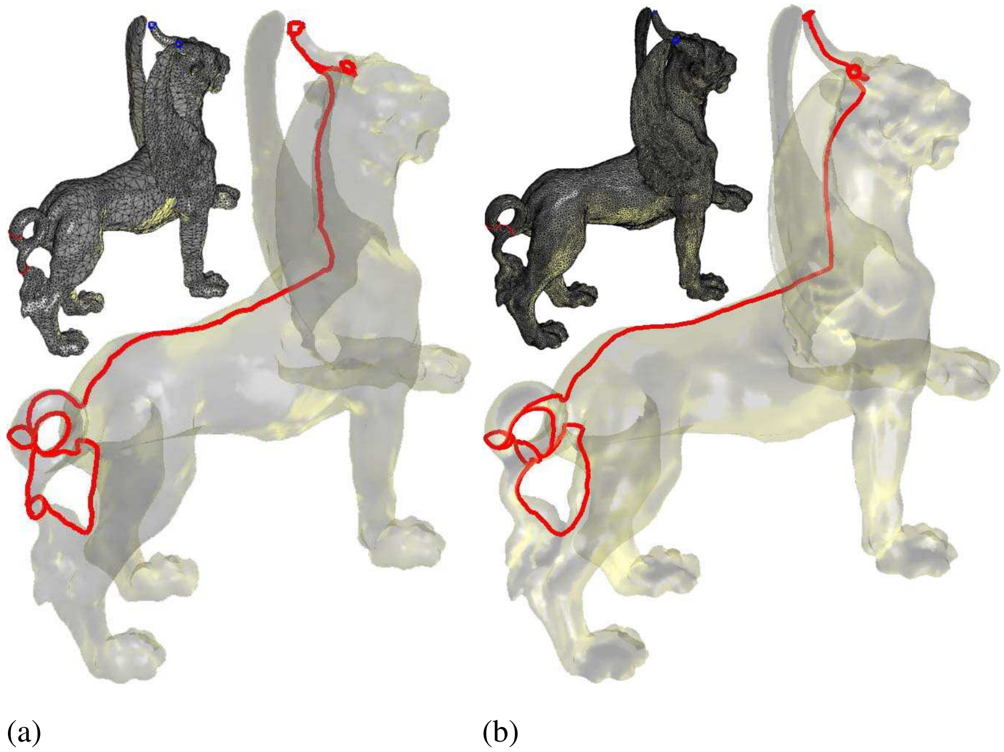

Fig. 12. Cut-graph on a (a) coarse and (b) refined surface of genus two with two boundary components located on the horns of the feline (blue curves); f is the geodesic distance from curvature extrema.

Γ_i^{-1}, we conclude that the polygonal schema has $2(\bar{b}-1)$ identified edges corresponding to the pairs (Γ_i,Γ_i^{-1}) and γ_i has been subdivided by Γ_i into two sub-parts $\gamma_i^{'}$, $\gamma_i^{''}$ such that $\gamma_i^{'}\cup\gamma_i^{''}=\gamma_i$. Therefore, the polygonal schema of $\mathcal{M}$ is

$$\gamma_1\Gamma_1\gamma_2^{'}\Gamma_2\gamma_3^{'}\ldots\gamma_{\bar{b}-1}^{'}\Gamma_{\bar{b}}\gamma_{\bar{b}}^{'}\Gamma_{\bar{b}}^{-1}\gamma_{\bar{b}-1}^{''}\ldots\gamma_2^{''}\Gamma_1^{-1}$$

which corresponds to a $(4\bar{b}-4)$-sided polygon. From (1), it follows that if $g=0$ the polygonal schema has $b-2$ redundant edges, and if $g\geq 1$ this schema is not canonical but it has a constant number (*i.e.*, $4g+b-4$) of redundant edges.

Joining boundary components with a given source point. The search of the canonical schema of $\mathcal{M}$ requires that each link path interpolates a given point $\mathbf{s}\in\mathcal{M}$. Let us suppose that $\mathbf{p}$ is the counterpart of $\mathbf{s}$ on the parameterization domain. At each step, the search of the shortest cut is constrained to join $\mathbf{p}$ to its closest boundary component with respect to the Euclidean distance. In this case, all the link paths share a common point $\mathbf{p}\in\gamma_1$; therefore, the polygonal schema is

$$\gamma_1\Gamma_1\gamma_2\Gamma_1^{-1}\Gamma_2\gamma_3\Gamma_2^{-1}\ldots\Gamma_{\bar{b}-1}\gamma_{\bar{b}}\Gamma_{\bar{b}-1}^{-1}$$

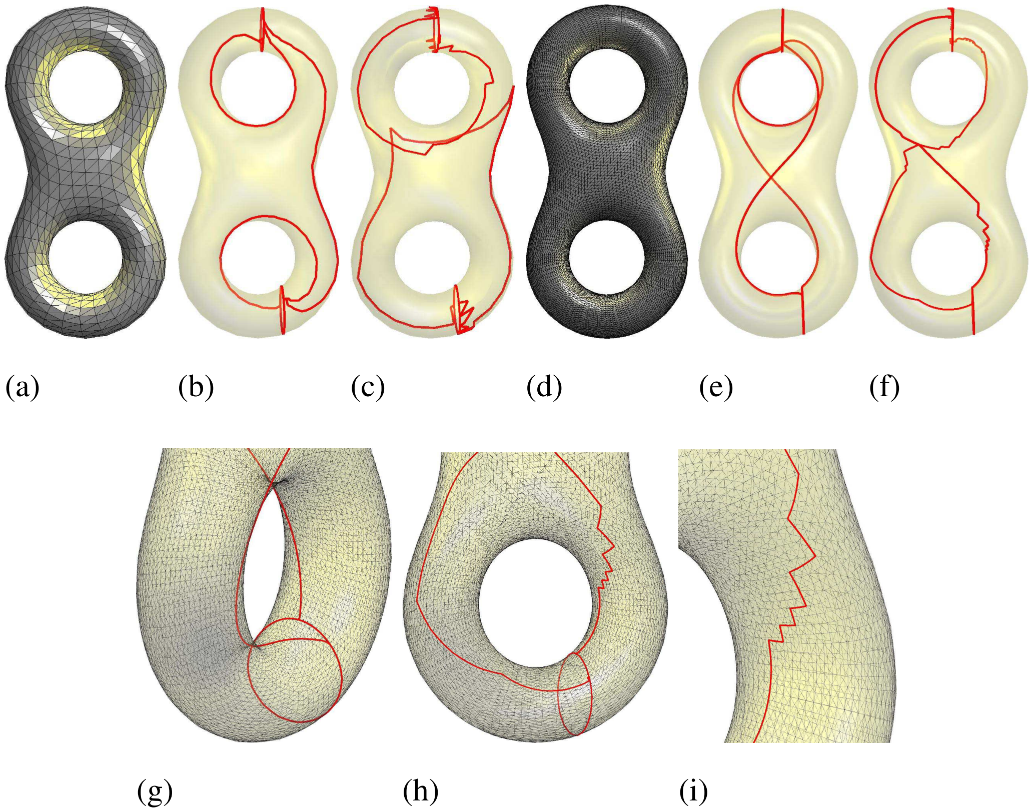

Fig. 13. Comparison of the cut-graph smoothness achieved by using the proposed approach and mesh-traversal techniques on the bitorus at two different levels of detail. (a) Coarse surface, (b) smooth cut-graph achieved by running the proposed approach, (c) geodesic cut-graph. (e-f) Counterparts of (b-c) on (d). (g) Zoom-in (e), (h-i) zoom-in (f).

which has $3b$ edges. The number of redundant edges is $2g$ and the schema is canonical if $g = 0$. However, the use of a base point can accumulate the parameterization distortion around $\mathbf{s}$ and therefore it may be not suitable for applications such as remeshing and texture mapping (see Fig. 6(c)).

3 Discussion

The proposed framework has three main degrees of flexibility: (a) the choice of the mapping function $f : \mathcal{M} \rightarrow \mathbb{R}$; (b) the selection of the meridian loops of the topological handles of $\mathcal{M}$; (c) the constraints on the procedure that builds the cut-graph. All these degrees of freedom define a *family of cut-graphs* for $\mathcal{M}$ (see Fig. 7 and 8). Furthermore, closed and bordered surfaces are treated with a unique approach which is stable with respect to the surface sampling and connectivity (compare Fig. 8 with 9 and see Fig. 10-12). The above-mentioned characteristics represent the main novelties of the proposed approach with respect to the state of the art on the search of cut-graphs of arbitrary triangle meshes. In the following, we discuss a

(a) (b)

Fig. 14. (a) Meridian loops of a 8-genus surface with topological handles of different shape and (b) related cut-graph; f is the second eigenfunction of the Laplacian matrix (Dong et al., 2006).

set of criteria for their selection and the effects on the resulting cut-graphs. Even thought the method used to identify and cut the topological handles of $\mathcal{M}$ is independent of the choice of the mapping function f, each f produces

- a different set of iso-contours, which are included in the cut-graph as meridian loops (see Fig. 4). For instance, the height function is useful if the input shape has a naturally privileged direction and the geodesic distance from source points is appropriate if the topological handles are part of protrusions or elongated features of the input shape. Fig. 6(b) and 13(e) show two cut-graphs whose meridian loops are the iso-contours of these mapping functions. As shown in Fig. 7 and 8, moving the meridian loop along the topological handle of $\mathcal{M}$ without affecting its global shape gives a family of cut-graphs with a similar shape. In general, a change of the shape or position of the handle cut will result in a different cut-graph and we are not able to predict the influence of the selected meridian cuts on the final result (see Fig. 11);
- a different number $m \geq 2$ of terminal arcs in the Reeb graph, or equivalently of critical points (see Fig. 4). Since the identification of the topological handles of $\mathcal{M}$ uses the combinatorial structure of the Reeb graph R_G, the computational cost for visiting R_G can be optimized by constructing a harmonic scalar field f on $\mathcal{M}$ with one minimum and maximum (Ni et al., 2004), and corresponding to a Reeb graph with two terminal nodes.

From the previous discussion, it follows that the best choice of f consists of selecting a scalar field which takes into account the shape of $\mathcal{M}$, has a low number of critical points, and does not require user-interaction for the selection of local extrema (resp., source points) as necessary for harmonic (resp., geodesic) mapping functions. The eigenvectors related to the smallest eigenvalues of the Laplacian ma-

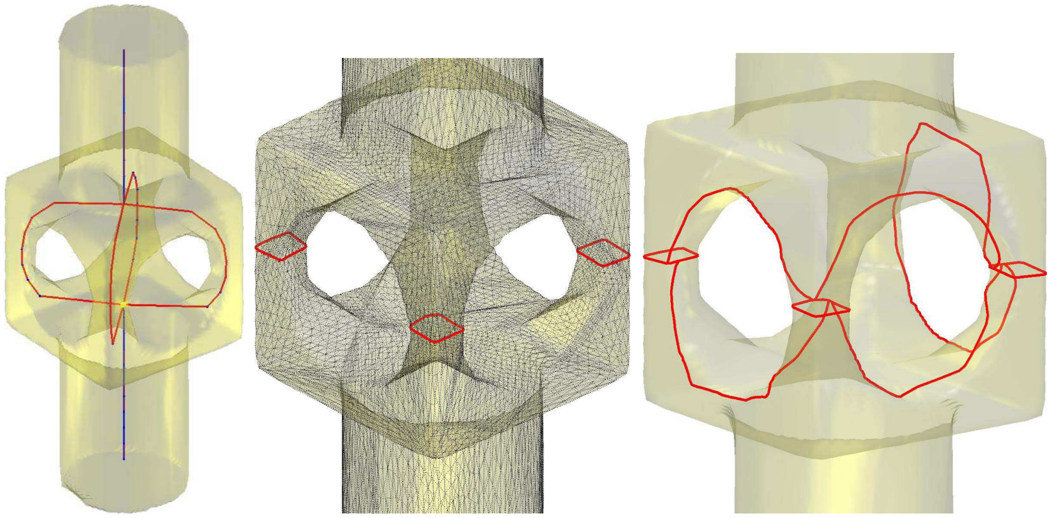

(a) (b) (c)

Fig. 15. (a) Reeb graph with respect to the height function of a surface of genus three, (b) cuts of the topological handles, and (c) cut-graph which is the best compromise between minimal length and parameterization distortion.

trix (2) associated to $\mathcal{M}$ have been recently used in (Dong et al., 2006) for quadrilateral remeshing and they have useful properties for our approach. In fact, since each one of these scalar fields is an eigenvector of the Laplacian matrix it takes into account both the geometric and topological aspects of $\mathcal{M}$ while maintaining a low number of critical points. Therefore, these eigenfunctions satisfy the above-mentioned criteria and they are natural choices if the harmonicity of f is not strictly required (see Fig. 4(e-h)). However, we note that this class of functions does not take into account the parameterization distortion of the embedding. Fig. 14 shows the meridian loops and the cut-graph of a surface of complex shape with respect to the second eigenvector of the Laplacian matrix; in this case, f has 4 maxima, 6 minima, and 24 saddles.

The iterative approach to the unfolding does not need to check if self-intersections of the cut disconnect the surface and it can also be applied to $\mathcal{M}$ without switching to the parameterization plane as discussed in Section 2.2. In this case, at the first step we select the longest boundary component which is then joined to its closest one by the shortest path. These two boundaries are then merged into γ and we set the weights of the edges in γ equal to $+\infty$. This update avoids that the next link paths will cross the cut found at the previous steps; then, the following iterations proceed as previously discussed. A more general strategy consists of defining γ as the minimum of the functional which is a convex combination between the cut length and the related parameterization stretch; this choice avoids having long and visible seams on the remeshed/textured surface while guaranteeing a low distortion.

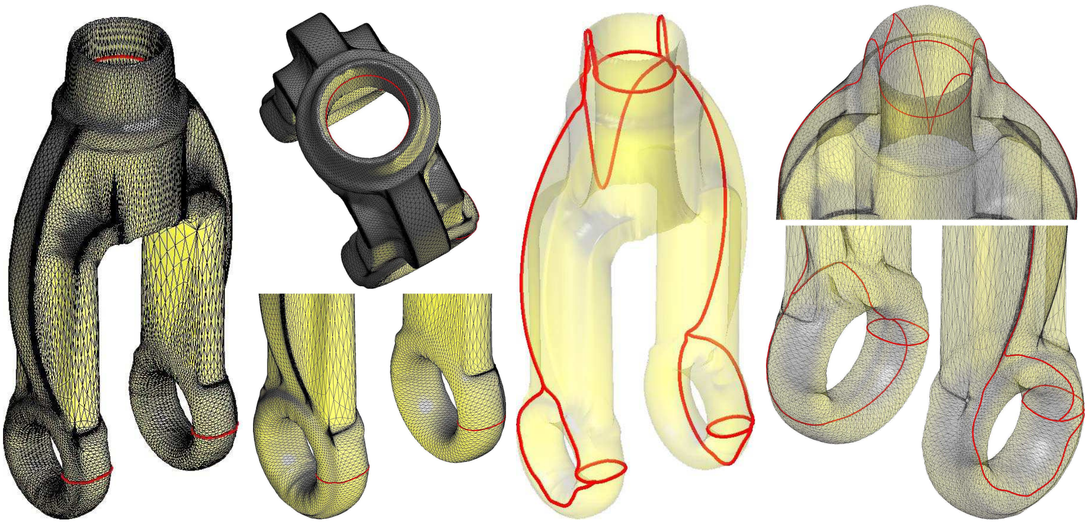

(a) (b) (c) (d)

Fig. 16. (a-b) Cut loops around the topological handles of a surface with genus three (f is the height function), (c) cut-graph, and (d) zoom-in.

Each link path is achieved by running the Dijkstra's algorithm on $\mathcal{D}$ with weights

$$\rho_{ij} = \lambda\rho_{ij}^{(g)} + (1-\lambda)\rho_{ij}^{(s)\,3}$$

where (i,j) is an edge of T, $\lambda \in [0,1]$, $\rho_{ij}^{(g)} := \|\mathbf{p}_i - \mathbf{p}_j\|_2$ is the edge length on $\mathcal{M}$, and $\rho_{ij}^{(s)} := (s_{ij}^{(1)} + s_{ij}^{(2)})^{-1}$ is the average of the L^2-stretch of the two triangles which share the edge (i,j) with respect to the current ϕ (see Fig. 15). As shown in Fig. 13(c,f,h-i), dealing with smooth cut loops and a surface with regular connectivity does not ensure to build smooth cut-graphs. We conclude that joining the boundary components of $\mathcal{M}^\star$ with the minimum spanning tree is computationally expensive (*i.e.*, $O(n\log(n))$), sensible to local noise, and the result depends on the input simplicial complex. Furthermore, the algorithm can compute paths which are different from true geodesic curves; this is because it takes shortcuts passing through edges instead of faces. In the examples shown in Fig. 13 and 15, we have normalized the two terms $\rho_{ij}^{(g)}$ and $\rho_{ij}^{(s)}$ in $[0,1]$ and set $\lambda = 1/2$. From the previous discussion, it follows that this last approach represents the geometric counterpart of the purely topological procedure discussed in Section 2.2. Since they cannot be included in a unique framework, in the following of this paragraph we propose to build γ through a 2-steps' approach which considers at first the topological aspects of the cut-graph search and then the geometric ones. In this way, we guarantee the smoothness of the cut-graph and the reduction of the distortion that the topological approach would produce.

[3] If $\lambda = 1$, we are using the approach previously discussed.

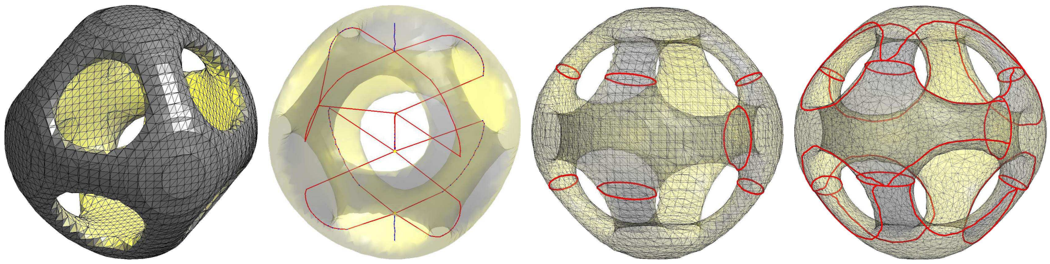

(a) (b) (c) (d)

Fig. 17. (a) Input surface of genus five, (b) Reeb graph with respect to the integral geodesic distance, (c) cuts of its topological handles, (d) cut-graph.

If the cut-graph γ is used for remeshing and texture mapping, two basic and conflicting constraints on its shape are the minimal length and a low parameterization distortion. The intuition of the following criteria is that short meridian loops and cut-graphs reduce the visibility of the seam on the remeshed/textured surface while selecting longer meridian loops and interpolating protrusions of $\mathcal{M}$ experience a lower stretch in the embedding of $\mathcal{M}$. For targeting the first aim, during the extraction of the Reeb graph R_G we identify the meridian loop of minimal length among all possible handle iso-contours of each arc in R_G; then, we build an initial cut-graph $\gamma^\star$ as described in Section 2.2. Since the search of the cut-graph which has minimal length would require to run the procedure for each possible set of handle cuts, we consider the shortest meridian loop along a given branch $\mathcal{B}$ of R_G and among the iso-contours that have been used to build $\mathcal{B}$, without using local optimization schemes. Therefore, its choice is linear in the number of nodes of the branch; the only caution is that its selection might be affected by a low number of slices on the topological handle associated to $\mathcal{B}$. At this stage, $\gamma^\star$ takes into account the topology of $\mathcal{M}$ but ignores the curvature distribution on $\mathcal{M}$. If $\gamma^\star$ does not interpolate high curvature regions of $\mathcal{M}$, the L^2-stretch of the corresponding planar embedding $\varphi : \mathcal{M} \rightarrow \Omega$ may be too high for remeshing and texture mapping. In this case, the cut-graph can be updated by adding to $\gamma^\star$ new link paths which take into account high curvature regions of $\mathcal{M}$ (Gu et al., 2002) or visibility constraints (Sheffer and Hart, 2002). Tests described in Section 2.2 and Table 1 show that accepting bifurcations of the link paths, which join the meridian cuts and the boundary components of $\mathcal{M}$, enable to reduce the parameterization distortion with respect to the other two choices. Furthermore, we stress that remeshing techniques such as (Alliez et al., 2003) adapt the vertex sampling to the local distortion of the embedding through the use of area-based density functions.

Each parameterization $\varphi : \mathcal{M} \rightarrow \Omega$ with respect to γ maps the cut to the regular approximation of the boundary of a planar polygon (*e.g.*, the unit circle or square); therefore, an important property of γ is its smoothness. A link path computed using the Dijkstra's algorithm is C^0, and actually it is a polyline made of edges of $\mathcal{M}$, while a path $\Gamma(\lambda) := \phi^{-1}(\lambda\mathbf{p} + (1-\lambda)\mathbf{q})$, $\lambda \in [0,1]$, is a piecewise linear approx-

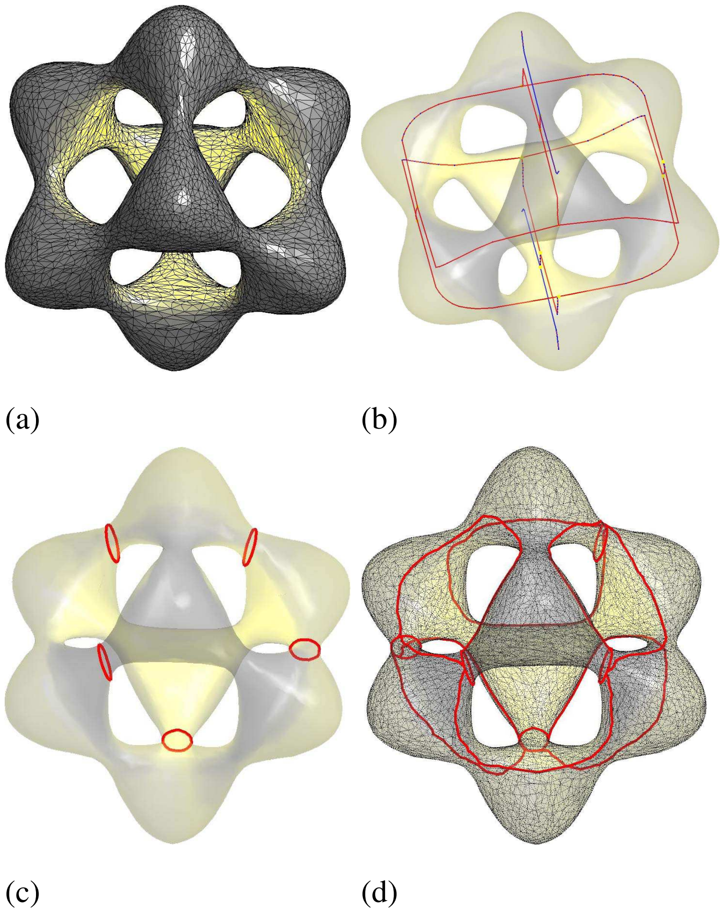

Fig. 18. (a) Input data set achieved by poligonizing an implicit surface, (b) Reeb graph with respect to the integral geodesic distance, (c) meridian loops constrained to have approximately the same length in order to reflect the symmetry of the surface, and (d) cut-graph.

imation of a path of class C^s if $\phi^{-1} \in C^s$ with the exception of the points where it intersects the other boundary components and the meridian loops, or where bifurcations occur. In these points a C^0-regularity holds (see Fig. 13). If we consider the parameterization ϕ with respect to harmonic weights, ϕ is the solution of the Laplacian equation $\Delta\phi = 0$ and $s \geq 2$; therefore, each link path of γ approximates a C^2 curve almost everywhere. Additional examples are given in Fig. 16-19 and timings are reported in Table 1.

4 Conclusions and future work

We discussed a computational method for calculating a family of cut-graphs of surfaces with boundary and an arbitrary genus proving that it extracts reduced polygonal schema if $g = 0$, and with a constant number or redundant edges if $g \geq 1$. In this last case, it is possible to convert redundant cut-graphs to a canonical form by applying standard reduction operations (Vegter and Yap, 1990). The proposed

Table 1
Timings (s:ms) include the evaluation of the Reeb graph, the identification of the meridian cuts, and the construction of the first cut-graph. Tests are performed on a Pentium IV 2.80 GHz.

Input	♯Vert.	g	b	Cut-graph	Input	♯Vert.	g	b	Cut-graph
Fig.2(d)	15320	9	0	14.12	Fig.12(a)	12563	2	2	10.52
Fig.6(a)	12286	2	0	1.14	Fig.12(b)	49864	2	2	51.12
Fig.6(b)	12286	2	0	1.21	Fig.15	8588	3	0	8.45
Fig.6(c)	12286	2	0	1.53	Fig.16	33233	3	0	37.01
Fig.7(c)	10044	1	0	8.51	Fig.18	15408	5	0	16.01
Fig.7(f)	10044	1	0	9.54	Fig.17	5622	5	0	4.58
Fig.9(a)	4255	1	1	3.05	Fig.19	41160	5	0	47.33
Fig.9(b)	4255	1	2	3.45					

framework builds on the Reeb graph R_G which codes in a combinatorial structure the topology of a given surface $\mathcal{M}$ and stores additional information such as the critical points, the genus of $\mathcal{M}$ as number of cycles, and the iso-contours of $(\mathcal{M}, f)$. In the same way, a cut-graph γ is an alternative high-level representation of $\mathcal{M}$ whose genus and boundary components correspond to a set of loops and link paths together with geometric properties such as minimal length and interpolation of a given source point. If we suppose that $\mathcal{M}$ is an arbitrary triangle mesh, R_G has k loops, $k \geq g$, while the cut-graph contains $2g$ loops related to g iso-contours (*i.e.*, meridians) of $(\mathcal{M}, f)$. The way these loops are joined can be different and the resulting link paths are not along each topological handle (*i.e.*, longitude). Therefore, the most interesting extension of our work consists of evaluating a homology base of an arbitrary surface $\mathcal{M}$ and it is based on the possibility of mapping the surface $\mathcal{M}^\star$ to a planar domain whose internal boundary components are constrained to have a pre-defined position on the parameterization domain.

Acknowledgments. This work has been supported by the EC-IST FP6 Network of Excellence "AIM@SHAPE". Special thanks are given to Silvia Biasotti for providing the Extended Reeb Graph code, to Rhaleb Zayer (MPII) for the quasi-harmonic parameterization tool, and to the anonymous reviewers for their constructive suggestions. Models are courtesy of the AIM@SHAPE repository. A video is available at the URL:
http://www.ge.imati.cnr.it/ima/smg/paragraph-web/Para-graph.html

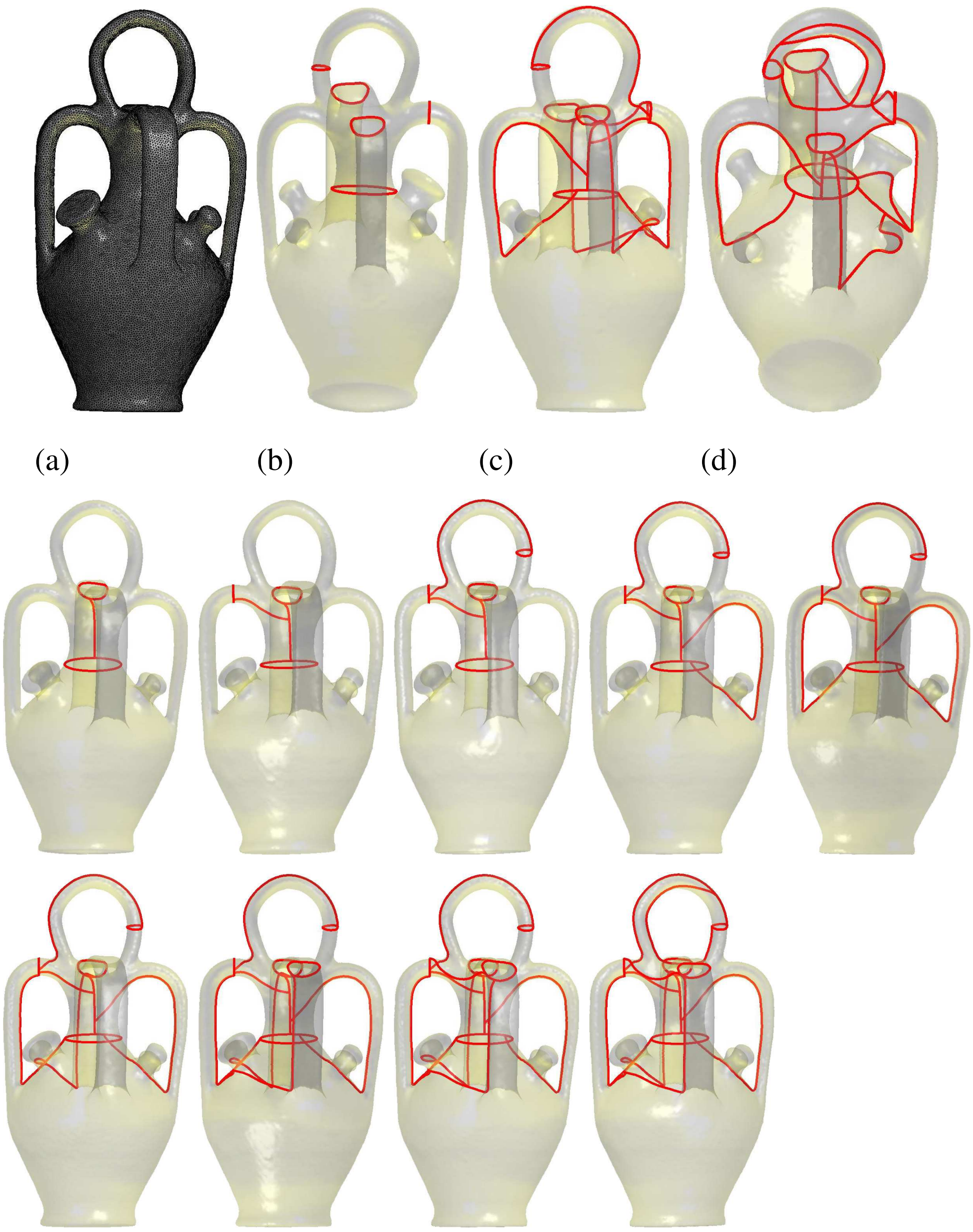

Fig. 19. First row: (a) input surface of genus five, (b) meridian loops, (c-d) two views on the cut-graph. Second and third row: steps of the iterative procedure which converts the surface (b) of 0-genus with ten boundary components into a disc-like surface while building its cut-graph.

References

Alliez, P., De Verdière, É. C., Devillers, O., Isenburg, M., 2003. Isotropic surface remeshing. In: Proceedings of Shape Modeling International. pp. 49–58.

Banchoff, T., 1967. Critical points and curvature for embedded polyhedra. Journal of Differential Geometry 1, 245–256.

Biasotti, S., May 2004. Computational topology methods for shape modelling ap-

plications. Ph.D. thesis, Universitá degli Studi di Genova.
Carr, H., Snoeyink, J., Axen, U., 2003. Computing contour trees in all dimensions. Comput. Geom. Theory Appl. 24 (2), 75–94.
Cole-McLaughlin, K., Edelsbrunner, H., Harer, J., Natarajan, V., Pascucci, V., 2003. Loops in reeb graphs of 2-manifolds. In: Proceedings of the nineteenth annual symposium on Computational geometry. ACM Press, pp. 344–350.
De Verdiere, E. C., Lazarus, F., 2002. Optimal system of loops on an orientable surface. In: Proceedings of the 43rd Symposium on Foundations of Computer Science. IEEE Computer Society, pp. 627–636.
Dijkstra, E., 1959. A note on two problems in connection with graphs. Numerical Mathematics 24 (1), 269–271.
Dong, S., Bremer, P.-T., Garland, M., Pascucci, V., Hart, J. C., 2006. Spectral surface quadrangulation. ACM Trans. Graph. 25 (3), 1057–1066.
Erickson, J., Har-Peled, S., 2002. Optimally cutting a surface into a disk. In: Proceedings of the eighteenth annual symposium on Computational geometry. ACM Press, pp. 244–253.
Erickson, J., Whittlesey, K., 2005. Greedy optimal homotopy and homology generators. In: SODA '05: Proceedings of the sixteenth annual ACM-SIAM symposium on Discrete algorithms. Society for Industrial and Applied Mathematics, Philadelphia, PA, USA, pp. 1038–1046.
Floater, M. S., 1997. Parametrization and smooth approximation of surface triangulations. Comput. Aided Geom. Des. 14 (3), 231–250.
Floater, M. S., 2003. Mean value coordinates. Comput. Aided Geom. Des. 20 (1), 19–27.
Floater, M. S., Hormann, K., 2005. Surface parameterization: a tutorial and survey. In: Dodgson, N. A., Floater, M. S., Sabin, M. A. (Eds.), Advances in Multiresolution for Geometric Modelling. Mathematics and Visualization. Springer, Berlin, Heidelberg, pp. 157–186.
Golub, G., VanLoan, G., 1989. Matrix Computations. John Hopkins University Press, 2nd. edition.
Gu, X., Gortler, S. J., Hoppe, H., 2002. Geometry images. In: Proceedings of the 29th annual conference on Computer graphics and interactive techniques. ACM Press, pp. 355–361.
Gu, X., Yau, S.-T., 2003. Global conformal surface parameterization. In: Proceedings of the Eurographics/ACM SIGGRAPH symposium on Geometry processing. Eurographics Association, pp. 127–137.
Hilaga, M., Shinagawa, Y., Kohmura, T., Kunii, T. L., 2001. Topology matching for fully automatic similarity estimation of 3D shapes. In: Proceedings of the 28th annual conference on Computer graphics and interactive techniques. ACM Press, pp. 203–212.
Kruskal, J., 1956. On the shortest spanning subtree of a graph and the traveling salesman problem. Proc. American Mathematical Society 7, 48–50.
Lazarus, F., Verroust, A., 1999. Level set diagrams of polyhedral objects. In: Proceedings of the fifth ACM Symposium on Solid Modeling and Applications. ACM Press, pp. 130–140.

Lopes, H., Tavares, G., Rossignac, J., Szymczak, A., Safanova, A., 2002. Edgebreaker: a simple compression for surfaces with handles. In: Proceedings of the seventh ACM symposium on Solid modeling and applications. ACM Press, pp. 289–296.

Massey, W. S., 1967. Algebraic Topology: An Introduction. Harbrace College Mathematics Series.

Milnor, J., 1963. Morse Theory. Vol. 51 of Annals of mathematics studies. Princeton University Press, Princeton.

Mortara, M., Patanè, G., 2002. Shape covering for skeleton extraction. International Journal of Shape Modelling 8 (2), 139–158.

Ni, X., Garland, M., Hart, J. C., 2004. Fair morse functions for extracting the topological structure of a surface mesh. ACM Trans. Graph. 23 (3), 613–622.

Pascucci, V., Cole-McLaughlin, K., 2002. Efficient computation of the topology of level sets. In: VIS '02: Proceedings of the conference on Visualization '02. IEEE Computer Society, Washington, DC, USA, pp. 187–194.

Patanè, G., Spagnuolo, M., Falcidieno, B., 2004. Para-graph: graph-based parameterization of triangle meshes with arbitrary genus. Computer Graphics Forum 23 (4), 783–797.

Pinkall, U., Polthier, K., 1993. Computing discrete minimal surfaces and their conjugates. Experimental Mathematics, 15–36.

Reeb, G., 1946. Sur les points singuliers d'une forme de pfaff completement integrable ou d'une fonction numerique. In: Comptes Rendu Acad. Sciences. Sciences Park, pp. 847–849.

Sheffer, A., Hart, J. C., 2002. Seamster: inconspicuous low-distortion texture seam layout. In: VIS '02: Proceedings of the conference on Visualization '02. IEEE Computer Society, Washington, DC, USA, pp. 291–298.

Sheffer, A., Levy, B., Mogilnitsky, M., Bogomyakov, A., 2005. Abf++: fast and robust angle based flattening. ACM Trans. Graph. 24 (2), 311–330.

Steiner, D., Fischer, A., 2002a. Cutting 3D freeform objects with genus-n into single boundary surfaces using topological graphs. In: Symposium on Solid Modeling and Applications. pp. 336–343.

Steiner, D., Fischer, A., 2002b. Growing surface methods for cutting 3d freeform objects with genus-n. In: Bi-National UK-Israel Conference on "Geometric Modeling Methods".

Steiner, D., Fischer, A., 2004. Planar parameterization for closed manifolds genus-1 meshes. In: Proceedings of the ninth ACM symposium on Solid modeling and applications. Blackwell Plubisher, pp. 83–92.

Vegter, G., Yap, C. K., 1990. Computational complexity of combinatorial surfaces. In: Proceedings of the sixth annual symposium on Computational geometry. ACM Press, pp. 102–111.

Wood, Z., Hoppe, H., Desbrun, M., Schroeder, P., 2004. Removing excess topology from isosurfaces. ACM Trans. Graph. 23 (2), 190–208.

Zayer, R., Rössl, C., Seidel, H.-P., 2005. Setting the boundary free: A composite approach to surface parameterization. In: Symposium on Geometry Processing. pp. 91–100.

Zhang, E., Mischaikow, K., Turk, G., 2005. Feature-based surface parameterization and texture mapping. ACM Trans. Graph. 24 (1), 1–27.